

# Statistical Study on the Thermodynamic Effect of Distant Disturbances Caused by Tropical Cyclones

Qinshuang SUN, Ju WANG\*, Tianju WANG, Yiyang PAN, Chenhan LIU, Zixuan WANG, Yicheng ZHOU

College of Meteorology and Oceanography, National University of Defense Technology, Changsha 410000, China

**Abstract** Multi-angle statistical analysis of tropical cyclones (TCs) and their distant thermodynamic disturbances over Northwest Pacific from July to September during 2001–2020 was conducted. The results show that TCs could trigger distant thermodynamic disturbances, which mainly caused an increase in air pressure and a rise in temperature in northern China. The distant thermodynamic disturbances triggered by TCs differed in spatial distribution and intensity in different months. In the same month, the spatial distribution of such disturbances triggered by high-intensity TCs was consistent with the overall pattern, and there was a significant increase in intensity and area. From the probability of TC activities and the significance test of variance of analysis under different levels of P–J index, it is found that TC activities could stimulate the increase of P–J teleconnection index. There was a significant positive correlation between them, which was accompanied by a step effect.

**Key words** Teleconnection quantity; Statistical analysis; Significance test; Distant disturbance; Thermodynamic effect

**DOI** 10.19547/j.issn2152–3940.2025.03.005

Tropical cyclones (TCs) occur frequently in China. The interaction between TCs and other weather systems such as westerly trough can lead to distant rainstorms. Research on distant rainstorms caused by TCs began with statistical analysis and case studies. For instance, Chen Lianshou<sup>[1]</sup> provided a clear definition of distant rainstorms caused by TCs, and found that distant rainstorms caused by TCs happened outside the range of TCs, and there was an intrinsic physical connection between rainstorms and TCs. Cong Chunhua *et al.*<sup>[2]</sup> pointed out that the water vapor transport of tropical cyclone (TC) circulation to a rainstorm area would lead to the convergence of water vapor in the rainstorm area, thereby enhancing the instability of atmospheric stratification. Observations show that the long cloud bands that often occur between TCs and the mid-latitude westerlies in autumn can last for several days. Such TC transporting heat and water vapor outward from the tropics can have a significant impact on westerlies circulation and weather, and also promote seasonal transitions, providing observational evidence that TC can affect weather-scale disturbances outside the tropics.

At the same time, since the weather-scale trough ridge of westerlies is manifested as the high- and low-value areas of geopotential height on the upper isobaric surface, the changes in the high- and low-value areas of geopotential height can be explained by the classical theory of dynamic meteorology. Moreover, the potential tendency equation indicates that the variation of geopotential height is mainly influenced by vorticity advection and temperature advection, and abnormal vorticity advection and temperature

advection will affect the development of the trough ridge system and the movement of flow patterns<sup>[3]</sup>. It provides an idea for studying the impact of TC activities on mid-latitude synoptic scale systems and a theoretical basis for studying the influence of TC-induced thermal disturbances on the tropical outer circulation.

Such TC activities can stimulate abnormal disturbances to propagate them into extra-tropical areas, and cause abnormal potential heights, vorticity and temperatures in middle latitudes, so they can affect the morphology and movement speed of westerly troughs at mid-latitude weather scales<sup>[4]</sup>. In terms of the influence of TC-induced abnormal disturbances on extra-tropical areas, Sun *et al.*<sup>[5]</sup> conducted a numerical test on sensitivity taking TC Megi (2010) as an example, the results show that the sinking and melting of ice crystals in the cloud anvons extending northwards in the upper layer of TCs will lead to the cooling of the lower tropospheric atmosphere in the tropics, resulting in a negative abnormal potential height. Wang Tianju *et al.*<sup>[6]</sup> found that the extra-tropical abnormal temperature and zonal wind caused by the TC activity generally satisfy the thermal wind relationship, and when the TC activity caused the meridional gradient of abnormal temperature, the zonal wind abnormally sheared with height. The results of these studies all indicate that TC activities over the tropical ocean surface can cause extra-tropical abnormal disturbances through multiple mechanisms, and thus should also have an impact on the characteristics of trough ridge activities at mid-latitude weather scales. In addition, Kawamura *et al.*<sup>[7]</sup> and Yamada *et al.*<sup>[8]</sup> respectively pointed out that TCs would effectively enhance tropical convection, resulting in abnormal meroidal wave lines from low latitudes to high latitudes, which could affect P–J teleconnection patterns and cause positive abnormal potential heights near Japan in middle latitudes. The numerical experiments conducted by Wang *et al.*<sup>[9]</sup> confirmed that the TC activity in the Northwest

Pacific can cause abnormal P – J teleconcorrelation phases and abnormal atmospheric disturbances near Japan in middle latitudes, resulting in abnormal positive geopotential height and abnormal subsidence movements, which is consistent with the results of Cha *et al.* [10]. This indicates that TCs affect P – J teleconcorrelation patterns to cause changes in extra-tropical circulation, which is an important form for the influence of TCs on extra-tropical circulation.

However, previous studies have not focused on the thermodynamic effects of distant disturbances caused by TCs, as well as the influence of distant thermodynamic disturbances excited by TCs on extra-tropical circulation, which limits the understanding and recognition of the feedback effect of TCs on extra-tropical circulation.

## 1 Materials and methods

NCEP/NCAR reanalysis data and data of typhoons over the Northwest Pacific from 2001 to 2020 from the China Typhoon Network were for statistical analysis. The reanalysis data covered data of multiple elements, with a time span of 2001 – 2020, a horizontal resolution of  $1^\circ \times 1^\circ$ , and a time resolution of 6 h, which provides data support for precise analysis.

Based on the reanalysis data, the TC activities in the Northwest Pacific in July, August and September over the past 20 years were statistically analyzed. The reanalysis data were classified based on the existence of TC activities in the Northwest Pacific. According to the classification results, synthetic analysis was carried out on physical quantities such as geopotential height, circulation, temperature and potential temperature, and then the synthetic average characteristics of each physical quantity in the two cases were obtained. Further, the physical quantities in the Northwest Pacific with TC activities were subtracted from those in the Northwest Pacific without TC activities. Thus, the statistical calculation results of distant thermodynamic disturbances induced by TCs were obtained to analyze their temporal variation characteristics and spatial distribution characteristics.

## 2 Analysis of statistical characteristics

TCs happen frequently in summer (July, August and September), and precipitation in China is most significantly affected by typhoons [11]. Therefore, the statistical characteristics of distant disturbances caused by TCs and P – J teleconcorrelation index in July, August and September were analyzed.

Firstly, TC activities from July to September over the past 20 years were statistically analyzed. The frequency of TC activities is shown in Fig. 1.

**2.1 Analysis of statistical characteristics of distant thermodynamic disturbances caused by TCs** From the fields of difference in geopotential height at 850 hPa in East Asia and the Northwest Pacific in two situations (with and without TC activity) (Fig. 2 – Fig. 4), it is found that in the area between  $30^\circ$  N and  $60^\circ$  N, the geopotential height in this area with TC activities was significantly higher than that without TC activity. From a statisti-

cal perspective, it can be proved that TC activities affected the geopotential height in middle latitudes. It was found that there were significant differences in the positive-value area of difference in various months. Among them, the positive-value area in July was significantly larger in both intensity and range than that in August and September, mainly existing between  $120^\circ$  –  $140^\circ$  E and  $30^\circ$  –  $60^\circ$  N. In July, August and September, the positive-value areas had obvious differences in the meridian direction, but were distributed in the mid-latitudes between  $30^\circ$  N and  $60^\circ$  N. As shown in Fig. 1, it can be known that the generation and activity areas of TCs were mainly located in the negative-value areas in low latitudes. Since TCs belonged to the low-pressure center, a strong negative-value area was bound to form in the area where they occurred frequently.

Based on the above analysis, the temperature anomaly and potential temperature anomaly in the mid-latitudes of East Asia with and without TC activities were further analyzed (Fig. 5 – Fig. 7). The positive-value area of difference in temperature was the strongest in intensity in August and was more concentrated in July and August, while the range was the largest but was relatively scattered in September. In July, August and September, there was a relatively obvious positive-value area of difference in temperature at  $100^\circ$  –  $120^\circ$  E and  $30^\circ$  –  $60^\circ$  N. From a statistical perspective, it can be concluded that TC activities may lead to an abnormal increase in temperature in this area. The intensity of both the positive-value and negative-value areas of difference in temperature in July was significantly weaker than that in August and September. The impact of TC activities on the temperature fields in East Asia and the Northwest Pacific in July was significantly weaker than that in August and September, which was contrary to the results of the geopotential height fields. In August, the positive-value area of difference in the temperature was roughly within the same range of  $100^\circ$  –  $120^\circ$  E and  $36^\circ$  –  $60^\circ$  N, mainly involving the northwest, north and northeast of China. It can be concluded that TC activities might cause high temperatures in the northwest, north and northeast of China in August. In the areas around  $120^\circ$  E and  $36^\circ$  N in September, there were double positive-value areas of difference in geopotential height and temperature. As TC activities occurred, high-temperature and high-pressure weather might occur in northern China.

**2.2 Statistical analysis of P – J teleconnection index and TC activities** The focus was on the distant thermodynamic effect of the enhancement of P – J teleconnection descending branch caused by TCs. Therefore, the P – J teleconnection index during different TC activity periods was mainly analyzed based on observational data, and the formula [12] is as follows.

$$PJI = [Z_{850}^*(155^\circ \text{ E}, 35^\circ \text{ N}) - Z_{850}^*(125^\circ \text{ E}, 25.5^\circ \text{ N})]$$

The maximum of P – J teleconnection index in each month was 281.247 1 (July 10, 2015), 234.876 3 (August 8, 2019), and 291.712 0 (September 5, 2019), respectively. Among the three values, it was the highest on September 5, 2019, and the descending branch of P – J teleconnection index was 1 575.87

gpm. The average in September was 1 540.32 gpm, and on that day, the descending branch of P – J teleconnection index ranked among the top 16% in the 20-year data. On September 4, the descending branch of P – J teleconnection index was 1 560.24 gpm. The descending branch of P – J teleconnection index on September 5 increased significantly compared to the previous day. Therefore, the P – J teleconnection index was up to the maximum on that day, which was affected by the increase in the descending branch of the P – J teleconnection index.

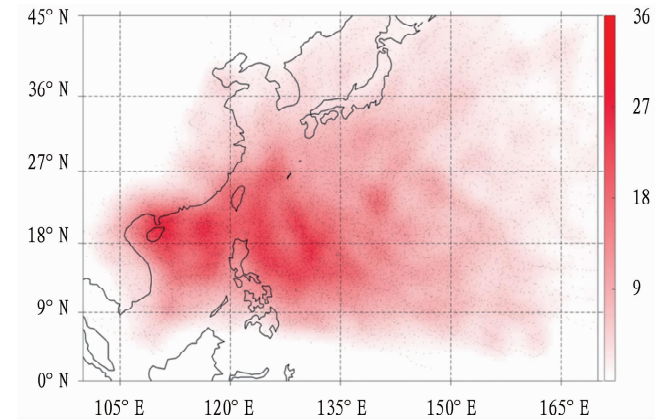


**Fig. 1** Frequency of TC activities during 2001 – 2020 (unit: K)

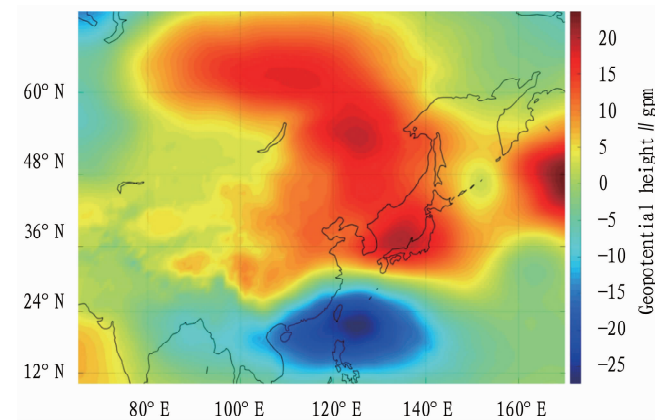


**Fig. 2** Field of difference in geopotential height at 850 hPa in July from 2001 to 2020

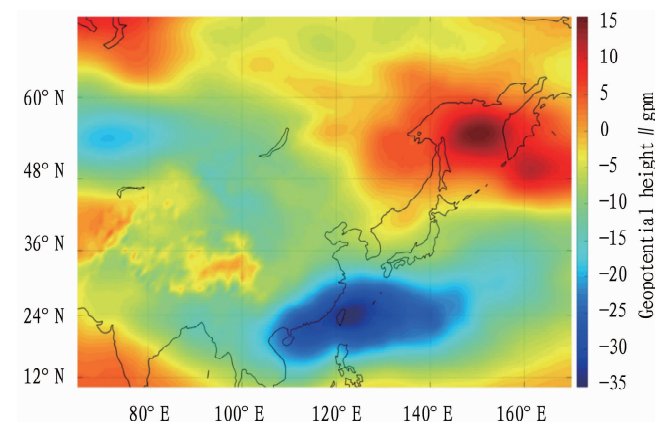


**Fig. 3** Field of difference in geopotential height at 850 hPa in August during 2001 – 2020

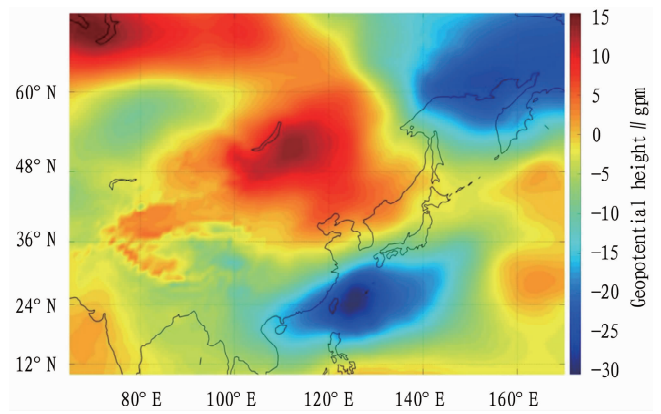


**Fig. 4** Field of difference in geopotential height at 850 hPa in September from 2001 to 2020

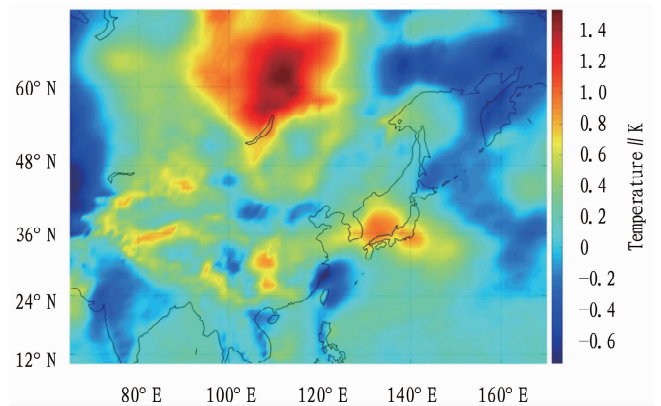


**Fig. 5** Field of difference in temperature at 850 hPa in July from 2001 to 2020

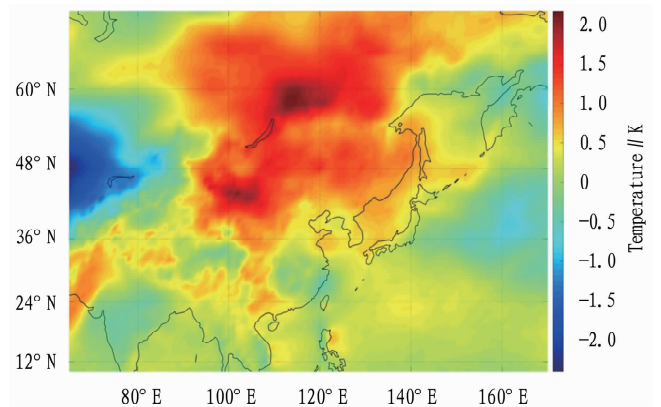


**Fig. 6** Field of difference in temperature at 850 hPa in August during 2001 – 2020

From the above analysis, it is found that in the same month from July to September, the probability of typhoons existing in the month with larger P – J teleconnection index was greater than that in the past twenty years (Table 1). Moreover, as the increase of P – J teleconnection index of the selected cases, the probability of the existence of typhoons was constantly increasing, even reaching 1. Therefore, it can be initially concluded that there was a correlation between typhoon activities and the increase of P – J teleconnection index.

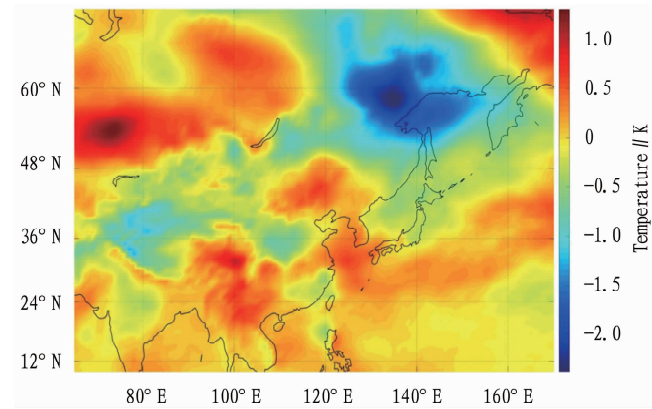


**Fig. 7** Field of difference in temperature at 850 hPa in September from 2001 to 2020

**Table 1** Changes in the probability of the existence of typhoons with the increase of P – J teleconnection index in July, August and September

Ranking of P – J teleconnection index	Probability of the existence of typhoons		
	July	August	September
In the past twenty years	0.66	0.86	0.85
Top 400	0.69	0.88	0.87
Top 200	0.72	0.95	0.95
Top 100	0.77	0.95	0.98
Top 50	0.80	0.96	1.00
Top 25	0.92	1.00	1.00

In order to further study the relationship between TC activities and P – J telecorrelation index, according to the different levels of the strongest TCs in the Northwest Pacific, they were divided into 7 grades: no typhoon, tropical depression, tropical storm, strong tropical storm, typhoon, strong typhoon, and super typhoon, and the significance of the correlation between TC activities and P – J telecorrelation index was tested by using the method of analysis of variance<sup>[13]</sup>.

**Analysis of variance:** factor  $x$  is grouped, and the grouping of  $y$  is also determined by the grouping of  $x$ . If the difference within a group of  $y$  is small but the difference between various groups is large,  $y$  is greatly influenced by factor  $x$ .

The sum of squares of the differences between groups is  $Q_1 = \sum_{j=1}^b \sum_{i=1}^a (\bar{y}_j - \bar{y})^2$ , while that within a group is  $Q_2 = \sum_{j=1}^b \sum_{i=1}^a (y_{ij} - \bar{y}_j)^2$ , where  $b$  represents the number of groups, and  $a$  means the number of elements within a group.

**F test:** hypothesis  $H_0$  that the influence of  $x$  on  $y$  is not significant was proposed. Statistic  $F = \frac{Q_1/(b-1)}{Q_2/(n-b)}$  was constructed, and the critical value  $F_\alpha$  was obtained from the given reliability  $\alpha$  and the distribution table of  $F$ . Then statistic  $F$  was calculated from the sample value, and was compared with  $F_\alpha$  to determine whether the hypothesis holds true.

The test results of statistic  $F$  show that it was 11.6 in July, 4.3 in August, and 18.0 in September, and  $F_\alpha$  was 2.1.

It can be seen from the results of the statistical test that at a confidence level of 95%, the strongest TCs existing in the North-

west Pacific in July, August and September had a significant impact on P – J telecorrelation index (Fig. 8 – Fig. 10). From the relationship between the grouping of TC intensity and the average of P – J telecorrelation index in July and September, it can be

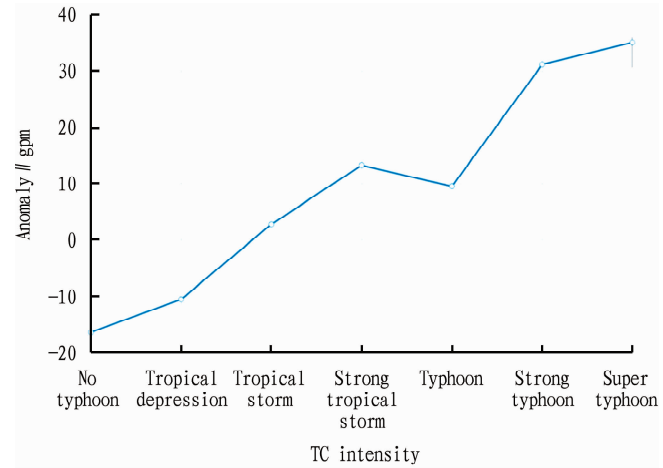


**Fig. 8** Relationship between TC intensity and P – J telecorrelation index in July

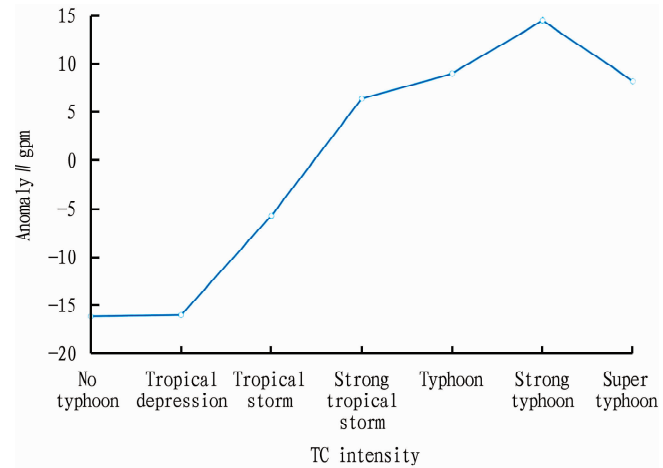


**Fig. 9** Relationship between TC intensity and P – J telecorrelation index in August

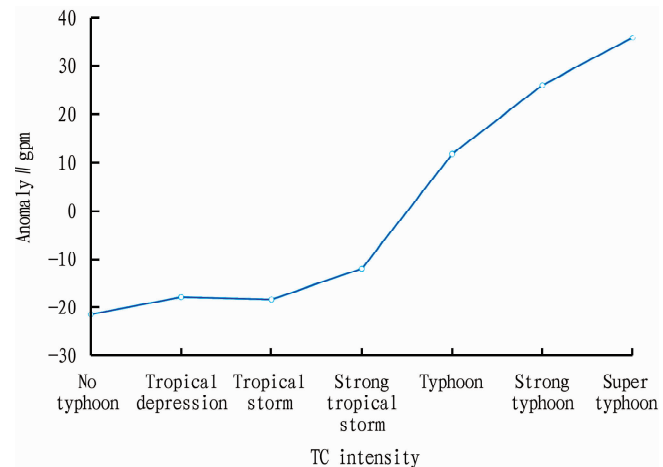


**Fig. 10** Relationship between TC intensity and P – J telecorrelation index in September



seen that there was an obvious linear relationship between the two. With the increase of TC intensity,  $P - J$  teleconcorrelation index approximately tended to increase linearly. In August,  $P - J$  teleconcorrelation index in the low-grade TC group was low, while  $P - J$  teleconcorrelation index in the high-grade TC group remained at a high level. Moreover, the average of  $P - J$  teleconcorrelation index in the super typhoon group was 40 in July and September, while in August, the average of  $P - J$  teleconcorrelation index was 10 in the super typhoon group and 15 in the strong typhoon group, which was significantly lower than that in July and September. It may be related to the differences in circulation patterns in July, August and September, which needs to be studied further.

**2.3 Statistical analysis of distant thermodynamic disturbances for different levels of TCs** From the statistical analysis of  $P - J$  teleconcorrelation index, it can be obtained that when TC reached typhoon and higher intensity, there was a significant increase in  $P - J$  teleconcorrelation index compared to lower-level TCs. Thus, the statistical analysis of distant thermodynamic disturbances of TCs was conducted separately when TCs were typhoon, strong typhoon, and super typhoon.

The fields of difference in geopotential height in two situations (with and without TC activity) were compared with the fields with typhoon (Fig. 11 – Fig. 13). Since TCs became a stronger low-pressure center after reaching the typhoon level, the negative-value area corresponding to the high-frequency activity area of TCs would obviously be significantly enhanced. In terms of the difference in the positive-value area, the intensity and area of the latter were both greater than those of the former. In July and September, the positive-value area basically covered the temperate regions of East Asia, but the positive-value area in August was relatively further east compared to July and September. The overall spatial distribution of the two was consistent.

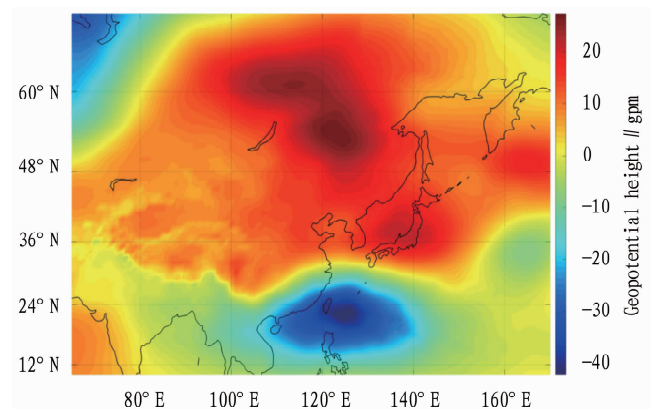


**Fig. 11** Field of difference in geopotential height at 850 hPa in July during 2001 – 2020

The fields of difference in temperature in two situations (with and without TC activity) were compared with the fields with typhoon (Fig. 14 – Fig. 16). It can be seen that the main positive-value and negative-value areas of the two roughly corresponded. However, the positive-value area of the latter was significantly stronger than the former in terms of area and intensity, and for the negative-value area, the intensity of the latter was also stronger

than that of the former. It indicates that the thermodynamic effect of distant disturbances of TCs was achieved by altering the temperature transport in East Asia, and this transport effect was positively correlated with the intensity of TCs. The differences in the intensity and area of the positive-value area in different months were consistent. That is, the intensity of the positive-value area was still the greatest in August, and the area of the positive-value area was the largest in September.

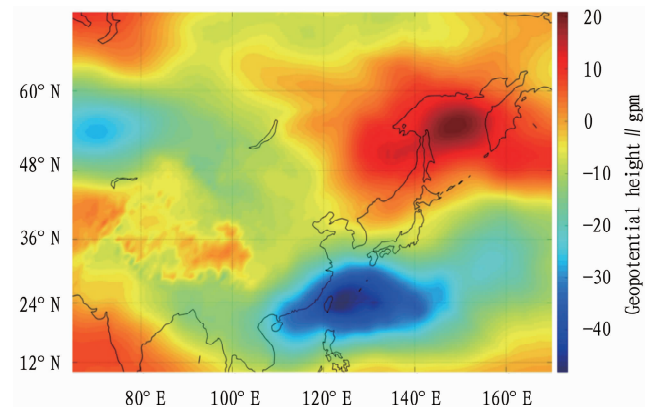


**Fig. 12** Field of difference in geopotential height at 850 hPa in August from 2001 to 2020

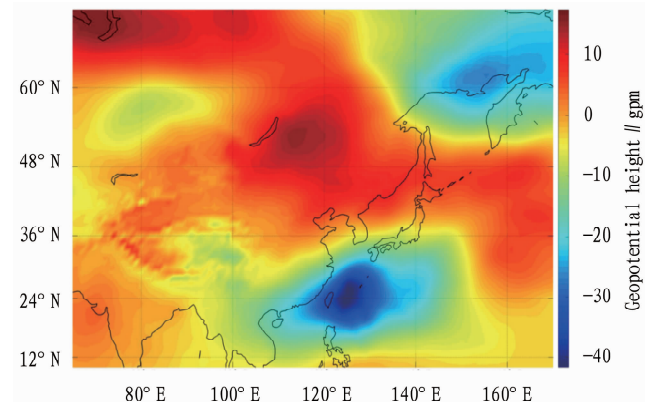


**Fig. 13** Field of difference in geopotential height at 850 hPa in September during 2001 – 2020

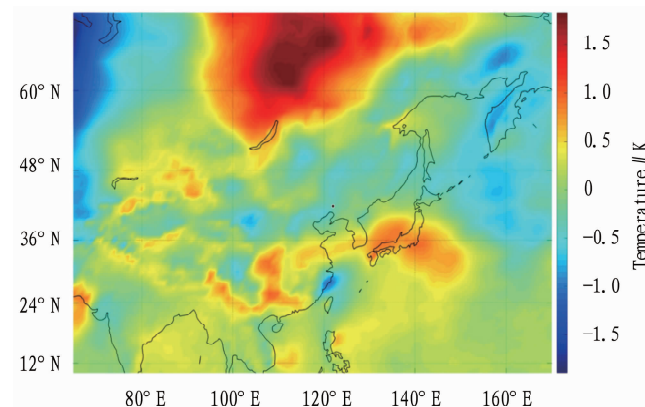


**Fig. 14** Field of difference in temperature at 850 hPa in July from 2001 to 2020

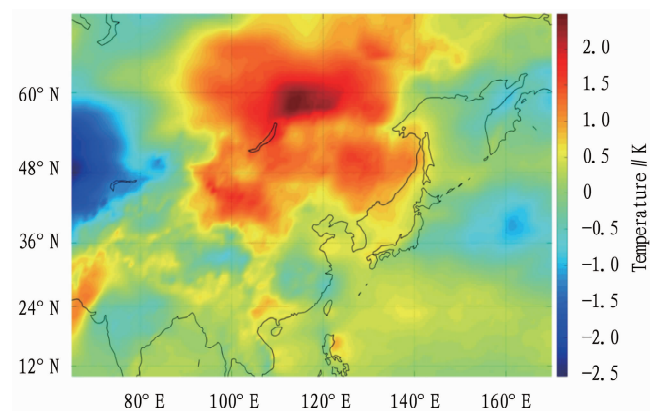


**Fig. 15** Field of difference in temperature at 850 hPa in August during 2001 – 2020

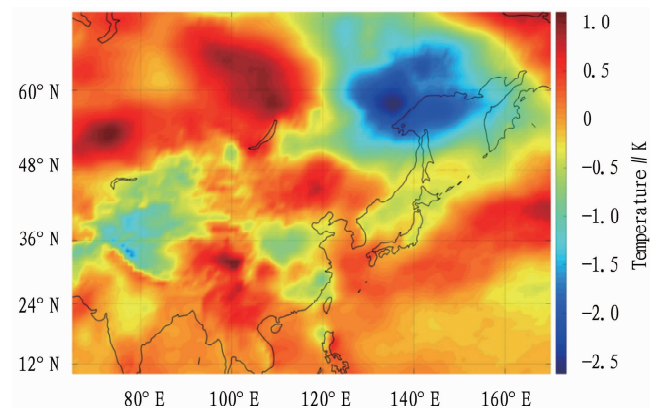


**Fig. 16** Field of difference in temperature at 850 hPa in September from 2001 to 2020

By comparing the fields of difference in geopotential height and temperature in the two groups, it can be concluded that the overall distribution of distant thermodynamic disturbances generated by high-intensity TCs were consistent. However, it is obvious that the distant thermodynamic disturbances generated by high-intensity TCs significantly increased in both intensity and range, and the difference in temperature in the high-frequency areas of TCs was not significant. The negative-value area of geopotential height fields was mainly generated by the low-pressure center characteristics of TCs. It can be concluded that the impact of distant thermodynamic disturbances caused by TCs on East Asia might be produced by affecting temperature and geopotential height transport, rather than directly transporting temperature and geopotential height to East Asia by TCs.

### 3 Conclusions

(1) TCs can trigger distant thermodynamic disturbances in East Asia, which can increase temperature and geopotential height. The distant thermodynamic disturbances triggered by TCs were achieved by altering the local temperature and geopotential height transport, and this effect was positively correlated with the intensity of TCs. There were significant spatial differences in the distant thermodynamic disturbances caused by TCs in different

months, while the impact of different intensities of TCs was consistent in overall spatial distribution.

(2) TC activities can lead to an increase in P – J teleconnection index, and there was a significant correlation between the two. The probability of TC activities when P – J teleconnection index was significantly higher than the overall probability of TC activities. As TC intensity reached typhoon level or above, the increase in P – J teleconnection index triggered would undergo a sudden change, and there was a significant increase compared to the increment of P – J teleconnection index caused by TCs at a low intensity level.

### References

- [1] CHEN LS. Research and forecasting of rainstorm caused by TCs [C]// The 14<sup>th</sup> National TC Science Symposium, 2007.
- [2] CONG CH. Research on long-distance rainstorms caused by tropical cyclones [D]. Beijing: Chinese Academy of Meteorological Sciences, 2011.
- [3] LIU YD, LYU MZ, GUO HL, *et al.* Dynamic meteorology [M]. Beijing: Meteorological Press, 2021.
- [4] WANG HW, FANG J. Analysis on a rainstorm related to remote typhoon during Meiyu period [J]. Journal of the Meteorological Sciences, 2014, 34(6): 601 – 611.
- [5] SUN Y, ZHONG Z, LU W, *et al.* Why are tropical cyclone tracks over the western North Pacific sensitive to the cumulus parameterization scheme in regional climate modeling: A case study for Megi (2010) [J]. Monthly Weather Review, 2014, 142(3): 1240 – 1249.
- [6] WANG TJ, ZHONG Z, WANG J, *et al.* Influence of tropical cyclone activities on the meridional movement of western Pacific subtropical high and its possible mechanisms: A case study [J]. Chinese Journal of Atmospheric Sciences, 2020, 44(4): 716 – 725.
- [7] KAWAMURA R, OGASAWARA T. On the role of typhoons in generating PJ teleconnection patterns over the western North Pacific in late summer [J]. SOLA, 200, 2: 37 – 40.
- [8] YAMADA K, KAWAMURA R. Dynamical link between typhoon activity and the PJ teleconnection pattern from early summer to autumn as revealed by the JRA – 25 reanalysis [J]. SOLA, 2007, 3: 65 – 68.
- [9] WANG T J, ZHONG Z, SUN Y, *et al.* 2019. Impacts of tropical cyclones on the meridional movement of the western Pacific subtropical high [J]. Atmospheric Science Letters, 2019, 20: e893.
- [10] CHA Y, CHOI JW, AHN JB. The interannual synchronization of the heatwave days in Korea and western North Pacific tropical cyclone genesis frequency [J]. International Journal of Climatology, 2022, 42(15): 1.
- [11] WANG X, ZHANG LF, WANG Y, *et al.* Influence of typhoons in the western Pacific on summer precipitation in the eastern Northwest China [J]. Chinese Journal of Atmospheric Sciences, 2024, 48(2): 507 – 520.
- [12] QIAN WH, LIANG HY. Atmospheric teleconnections and regional-scale atmospheric anomalies over the Northern Hemisphere [J]. Chinese Journal of Geophysics, 2012, 55(5): 1449 – 1461.
- [13] YAO LN, REN J, LUO ZX. Preliminary study on variations of landfalling tropical cyclone rainfall over East China [J]. Journal of Nanjing Institute of Meteorology, 2009, 32(1): 87 – 93.